Self-Assembled Periodical Polycrystalline-ZnO/a-C Nanolayers on Zn Nanowire

Quan Li* and K.W. Kwong

Department of Physics, The Chinese University of Hong Kong, Shatin, New Territory, Hong Kong, China

D. Ozkaya and D. J. H. Cockayne

Department of Materials, University of Oxford, Parks Road, Oxford OX1 3PH, United Kingdom

Zn nanowires with an epitaxial thin surface layer of zinc oxide were dispersed onto amorphous carbon films and stored at room temperature. After 1500 h, a self-organized equal-spaced zinc oxide ($\simeq$ 2 nm)/carbon ($\simeq$2.5 nm) multilayer structure was found to form outside the Zn nanowire, taking the place of the original ZnO surface layer. We carried a systematic study to clarify the self-formation mechanism of the periodical multilayers outside the Zn nanowire and found out that such a configuration originated from a chemical reaction between Zn and CO_2 and were formed via a gas phase diffusion—interfacial chemical reaction—phase separation process.

Self-assembly of nanosized domain patterns has attracted much attention in recent years due to its potential applications in nanodevices and in materials patterning at the nanometer scale. The reported self-organization processes include the formation of (i) metal [1] (metal alloy [2], semiconductor [3,4], etc.) domains on metal (metal alloy, semiconductor, etc.) surfaces, driven by surface-lattice dislocations [1] or by the stress field in the substrate around the individual domains [5–9], (ii) lateral multilayer superlattices of semiconductors [10] and metals [11,12] driven by the film/substrate interfacial strain-induced phase separation, and (iii) three-dimensional quantum dots produced during strained-layer epitaxial growth [13,14]. Almost all of these self-assembly processes require a certain mobility of the atoms, a stress (strain) field or other form of interatomic interactions (e.g., chemical bonding) as the driving force.

In this Letter, we report self-organized periodical zinc oxide/amorphous carbon (a-C) multilayers forming outside a Zn nanowire, with a periodicity of $\simeq$ 4.5 nm. The self-assembly process originates from chemical reaction between Zn and CO_2 and results in highly ordered multilayer nanostructures on the nanowire surface. This observation suggests the possibility of decorating nanowire surfaces with multilayer "coatings," which could largely modify the surface properties of the nanowires, including improved mechanical behavior and chemical inertness and stability of the nanowire.

Zn nanowires were synthesized by thermal reduction of zinc sulfide using hydrogen [15]. The first observation of the periodical multilayer structures outside the Zn nanowire was made accidentally on the Zn nanowires, which were dispersed onto carbon film (Ted-Pella Inc.) and then stored in air over 1500 h. Transmission electron microscopy (TEM) was employed to investigate the resulting nanowire structures and their chemical compositions. A JEOL 3000 FEG-TEM and a Tecnai 20

FEG-TEM were used for TEM imaging. X-ray spectroscopy and energy loss elemental mapping of the nanowires were performed using an energy dispersive x-ray (EDX) spectrometer (Oxford Instruments) and a Gatan imaging filter system attached to the microscopes.

EDX results suggest that the freshly synthesized nanowires are composed of Zn and O. Figure 1 shows a high resolution image of the freshly synthesized Zn nanowire with a selected area diffraction (SAD) pattern taken from
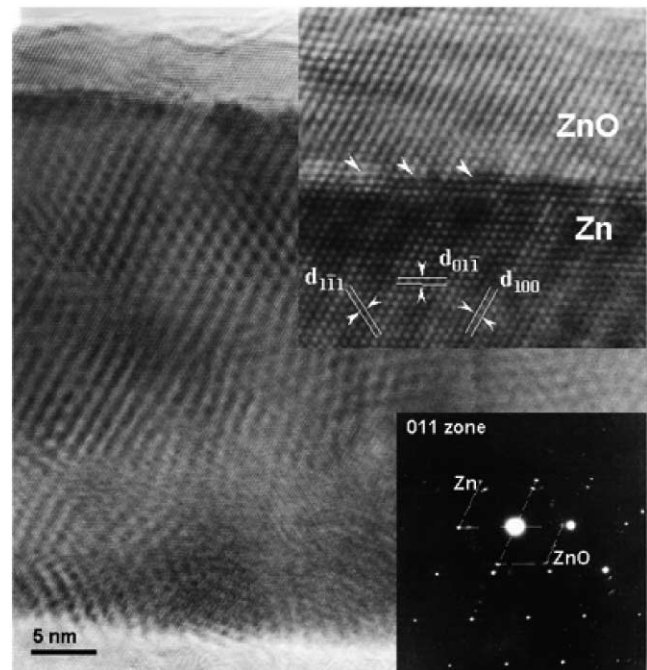

FIG. 1. High resolution TEM image of the freshly synthesized Zn nanowire; an epitaxial ZnO surface layer is observed. The selected area diffraction pattern in the inset further confirms the epitaxial relationship between Zn and ZnO seen in the image.

the same wire shown in the lower-right inset. The high resolution image and diffraction pattern indicate the hexagonal structure for both Zn and ZnO and epitaxy between them $\{[011]_{Zn}//[011]_{ZnO}, (100)_{Zn}//(100)_{ZnO}\}$. The Moiré fringes in the Zn-core region result from the overlapping of the Zn core and the ZnO sheath. In the enlarged high resolution image in the upper right inset of Fig. 1, extra planes (look like the end on misfit dislocations) appear at the Zn/ZnO interface every six Zn (100) planes (five ZnO planes) on average (marked by arrows).

As a comparison, Fig. 2 shows a Zn nanowire, which had been dispersed on carbon film and stored in air for 1500 h. Figure 2(a) is a low-magnification bright field (BF) image of the nanowire, showing light and dark striations in the surface layer. The high resolution image in Fig. 2(b) reveals a well-defined multilayer structure
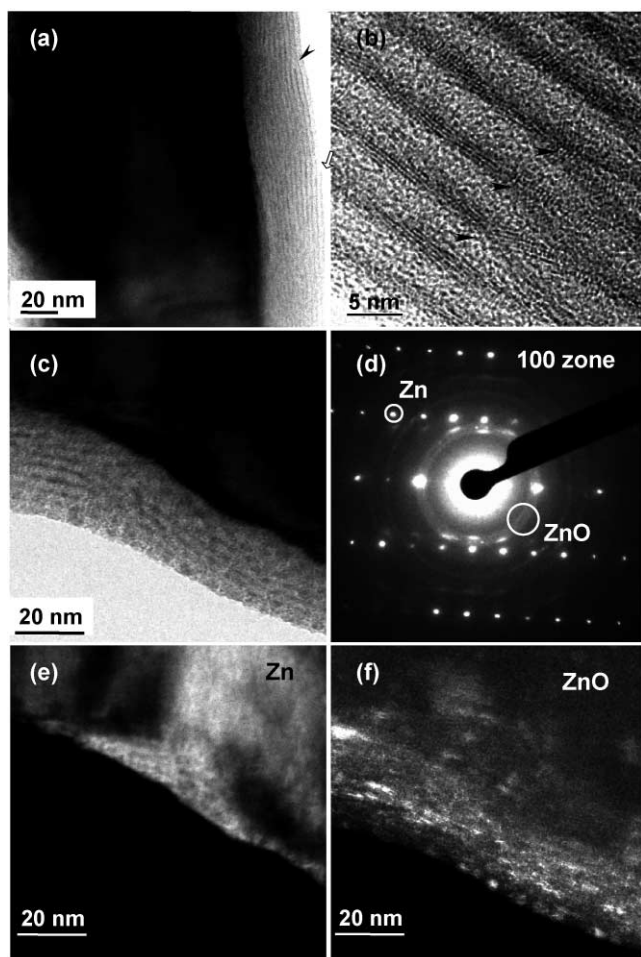

FIG. 2. (a) Bright-field image of a Zn nanowire stored on carbon film for 1500 h; periodic light/dark layer contrast is observed; (b) high resolution image showing an ordered nanolayer structure; (c) bright-field image of another Zn nanowire from the same sample; (d) SAD pattern taken from the nanowire shown in (c); (e) dark-field image formed from the diffraction spot from Zn; (f) dark-field image formed from part of the diffraction ring from ZnO.

in the surface layer outside the Zn core. The dark layer ($\simeq 2$ nm) appears to be polycrystalline, while the light layer ($\simeq 2.5$ nm) appears to be amorphous. Discontinuities of these nanowires are commonly observed [marked by arrows in Fig. 2(b)]. Over the several tens of nanowires examined, all of them had formed such multilayer surface nanostructures. The SAD pattern [Fig. 2(d)] taken from such wires [eg Fig. 2(c)] appears to be different from those from the freshly synthesized wires (Fig. 1). While the diffraction pattern from Zn shows sharp spots, the diffraction pattern from ZnO is in the form of a ring pattern. Dark field images taken by choosing a specific Zn diffraction spot or part of a ZnO diffraction ring [marked by white circles in Fig. 2(d)] indicate that Zn and ZnO are still located in the core [Fig. 2(e)] and shell areas [Fig. 2(f)], respectively. Figure 2(f) shows some layered contrast inside the shell region.

Figure 3 shows the BF zero-loss electron energy loss (EEL) map [Fig. 3(a)] of such a nanowire together with the EEL maps using the Zn L edge [Fig. 3(b)], carbon K edge [Fig. 3(c)], and oxygen K edge [Fig. 3(d)]. While both the Zn and C maps reveal modulated layer structures, oxygen appears to be more evenly distributed over the whole surface layer. Overlapping the chemical maps with the original BF image indicates a correlation between carbon and the light layer, and between Zn and the dark layer.

These experimental results suggest that an ordered polycrystalline-ZnO/a-C multilayer nanostructure is self-organized outside the Zn nanowire surface, taking the place of the original epitaxial single crystalline ZnO surface layer.
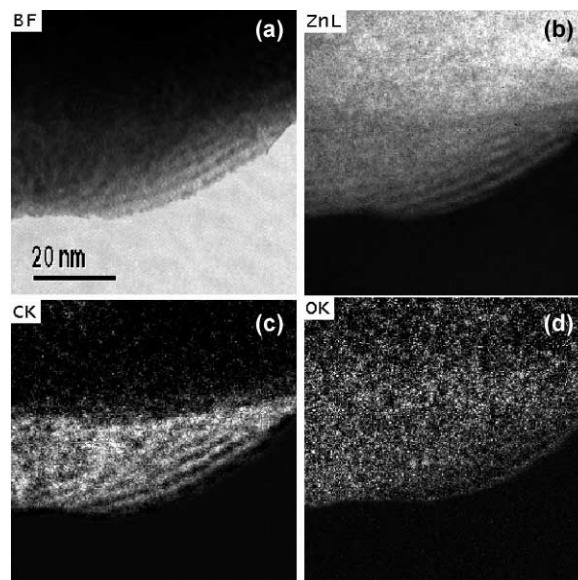

FIG. 3. (a) Bright-field image of part of the Zn nanowire with multilayer surface structure; (b) EELS map using the Zn L edge; (c) EELS map using the C K edge; (d) EELS map using the O K edge.

In order to find out the formation mechanism of the periodical multilayers, a series of experiments are designed to reproduce such multilayer structures outside the freshly synthesized Zn nanowires. First, we tried to identify the source of carbon in the multilayer structures. A thick carbon layer was deposited onto the fresh Zn nanowires before they were dispersed onto the carbon film. No multilayer structures were observed after six months, a result that suggested that the solid carbon phase wrapping the Zn nanowire, if not completely prevented, at least slowed down the multilayer formation to a large extend. This eliminates the possibility of solid phase carbon diffusion into the ZnO layer as the major driving force for the multilayer structure formation.

The freshly synthesized Zn nanowires were then placed into a gas reaction cell, using carbon dioxide as the flowing gas. A small amount of samples were taken out from the gas cell after different periods of reaction time and were immediately dispersed onto carbon films for TEM observations. The ordered multilayers outside the Zn core appear after $\simeq 150$ h, suggesting the effectiveness of this method in reproducing the multilayer structures. It is interesting to note the evolution of the outer sheath that wraps the Zn core. Starting from a thin ZnO layer (native oxide usually $\simeq 5$ nm in thickness), only one or two ill-shaped ZnO/C alternating layers appear at the outermost surface of the nanowire for samples in the gas cell up to 48 h [Fig. 4(a)]; several more multilayers appear at the outermost surface region of the nanowire together with small ZnO particles ($\simeq 2$ nm) embedded in an amorphous carbon ma-

trix sitting in between the ordered multilayers and the Zn-core/sheath interface [as marked by arrows in both Figs. 4(b) and 4(c)], for samples in the gas cell up to 150 h [Figs. 4(b) and 4(c)]; even more periodical multilayers can be observed for samples in the gas cell for longer hours [Fig. 4(d)]. Moreover, the total thickness of the ZnO in the multilayers becomes much larger [$\simeq 20$ nm in Fig. 4(d)] compared to that of a freshly synthesized Zn nanowire.

The above experimental results suggest that the carbon phase in the ZnO/C multilayers mainly come from the chemical reaction between Zn and CO_2,

$$Zn + CO_2 \rightarrow ZnO + C,$$
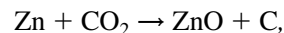
which is thermodynamically favorable at room temperature. CO_2 first diffuse to the Zn/ZnO interface of the freshly synthesized Zn nanowire, where they react with Zn leading to ZnO and C. Such a diffusion process may occur at a reasonable rate considering the cylindrical configuration of the nanowire; i.e., defects and grain boundaries are expected in the nanowire radial directions, providing an easy diffusion route for the gas molecules. We cannot exclude the possibility of bulk diffusion through the native ZnO layer, as this layer is formed by oxidation of the Zn surface, which process results in a Zn concentration gradient along the nanowire radial direction [16]. The ZnO layer is highly oxygen deficient. The Zn concentration gradient and the oxygen point defects may serve as the driving force for CO_2 diffusion through the lattice to react with Zn — a process similar to the oxidation of metallic Zn in air — but are expected to occur at low rates [16]. In fact, the oxidation reaction between Zn and O_2 is thermodynamically more favorable compared to that between Zn and CO_2. Nevertheless, our experiments were carried in 100% CO_2 atmosphere, which eliminates the possibility of direct reaction between Zn and O_2. Similarly, for the ZnO/C multilayers first observed in Zn nanowires dispersed on the carbon film, although we did not deliberately introduce any C containing gas, it was the CO_x enriched in the vicinity of the carbon film that served as the carbon source. As a comparison, only increased ZnO sheath thickness is observed for freestanding Zn nanowires stored in the ordinary atmosphere, where O_2 is the majority.

The chemical reaction at the Zn-core/sheath interface leads to the formation of C and ZnO, which two phases are immiscible. Phase separation would occur once a critical mass of the C and ZnO is reached, resulting in a ZnO-particle/amorphous C configuration in the vicinity of the Zn-core/sheath interfacial region [as shown in Fig. 4(b)]. As the chemical reaction continues at the Zn-core/sheath interface, ZnO and C are continuously produced at the interfacial region, pushing the original sheath materials away from the interface. The large interfacial area associated with the resulted
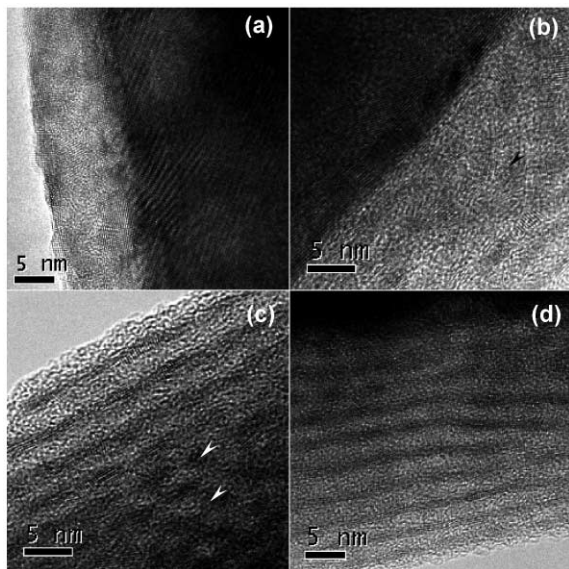

FIG. 4. High resolution TEM images showing the evolution of the native ZnO layer wrapping the Zn nanowire core after different reaction times in the gas cell. (a) For samples up to 48 h; (b),(c) for samples up to 150 h; (d) for samples with even longer hours.

ZnO-particle/amorphous carbon configuration is energetically unfavorable. To minimize the interfacial energy, together with the driving force generated by the ''pushing'' process, the ZnO particles align with each other in the short range, leading to the polycrystalline ZnO/amorphous C multilayer structures. The experimental fact that the size of the ZnO particle ($\simeq 2$ nm) is similar to the polycrystalline ZnO layer thickness ($\simeq 2$ nm) supports this argument. The inner layers of the whole sheath suffer more from the concentration change of both ZnO and C, when compared to the outer layer region. Such a dynamic process determines that the equilibrium is the first to reach the outermost surface of the nanowire (being the farthest away from the interfacial region), which becomes the first site for the ordered multilayer to appear [Fig. 4(a)]. Once the multilayers are formed at the outermost surface region, a further pushing process can be realized through pseudodislocation (discontinuous ZnO layers throughout the multilayer structures) movements without destroying the already formed multilayer structures. The pseudodislocations resemble the edge dislocations moving through a crystalline lattice during the plastic deformation and eventually terminate at the outer surface as ''surface step'' [marked by the open arrow in Fig. 2(a)]. Such pseudodislocation features are observed [marked by solid arrows in Figs. 2(a) and 2(b)] in all of the samples with the multilayer configurations.

We also found that the epitaxial relationship between the Zn core and the native ZnO layer is not critical for the multilayer formation, as similar experiments have been conducted using Zn nanowires with polycrystalline ZnO sheath, and multilayer structures are detected in an even shorter time duration. The observation is consistent with the gas molecule grain boundary diffusion argument as stated above.

In conclusion, we report the self-organization of the periodic polycrystalline-ZnO/a-C multilayer nanostructure outside the Zn nanowires. The structure and the chemical composition of the nanolayers have been unambiguously analyzed by TEM, EDX, and EELS. Unlike other reported self-assembly processes, where the surface stress (strain) field [1–9] or certain chemical force is mainly responsible for the stabilization of ordered structures, this system is rather complicated, which involves a gas phase diffusion, an interface chemical reaction followed by a phase separation, and a self-alignment process. The interfacial reaction and the resulting inner-out material movement, together with the immiscible nature of ZnO and C, are critical driving forces for the self-organization of periodical multilayer structures. Such a mechanism may be generally applied to other material

systems satisfying the above-mentioned criteria, leading to the self-assembly of ordered multilayer nanostructures, which may have various applications in nanotechnology [17] using these nanowires as various nanoprobes, nanosensors, etc.

*Corresponding author.
Electronic address: liquan@phy.cuhk.edu.hk

[1] D. D. Chambiliss, R. J. Wilson, and S. Chiang, Phys. Rev. Lett. **66**, 1721 (1991).
[2] R. Plass, J. A. Last, N. C. Bartelt, and G. L. Kellogg, Nature (London) **412**, 875 (2001).
[3] D. J. Eagelsham and M. Cerullo, Phys. Rev. Lett. **64**, 1943 (1990).
[4] D. Vanderbilt and L. K. Wickham, in *Evolution of Thin Film and Surface Microstructure*, MRS Symposia Proceedings No. 202 (Materials Research Society, Pittsburgh, 1991), p. 555.
[5] K. Pohl, M. C. Bartelt, J. de la Figuera, N. C. Bartelt, J. Hrbek, and R. Q. Hwang, Nature (London) **397**, 238 (1999).
[6] M. Seul and D. Andelman, Science **267**, 476 (1995).
[7] D. Vanderbilt, Surf. Sci. **268**, L300 (1992).
[8] K. O. Ng and D. Vanderbilt, Phys. Rev. B **52**, 2177 (1995).
[9] H. Ibach, Surf. Sci. Rep. **29**, 195 (1997).
[10] A. Zunger and S. Mahajan, in *Handbook of Semiconductors*, edited by T. S. Moss (Elsevier, Amsterdam, 1994), Vol. 3, p. 1399.
[11] E. D. Tober, R. F. C. Farrow, R. F. Marks, G. Witte, K. Kalki, and D. D. Chambliss, Phys. Rev. Lett. **81**, 1897 (1998).
[12] E. D. Tober, R. F. Marks, D. D. Chambliss, K. P. Roche, M. F. Toney, A. J. Kellock, and R. F. C. Farrow, Appl. Phys. Lett. **77**, 2728 (2000).
[13] J. Tersoff, C. Teichert, and M. G. Lagally, Phys. Rev. Lett. **76**, 1675 (1996).
[14] G. Springholz, V. Holy, M. Pinczolits, and G. Bauer, Science **282**, 734 (1998).
[15] J. Q. Hu, Q. Li, X. M. Meng, C. S. Lee, and S. T. Lee, Chem. Mater. **15**, 305 (2003).
[16] O. Kubaschewski and B. E. Hopkins, in *Oxidation of Metals and Alloys* (Butterworths, London, 1962), 2nd ed.
[17] J. Patscheider, MRS Bull. **28**, 180 (2003).